Evidence for Above-Surface and Subsurface Neutralization during Interactions of Highly Charged Ions with a Metal Target

F. W. Meyer, S. H. Overbury, C. C. Havener, P. A. Zeijlmans van Emmichoven, and D. M. Zehner
Oak Ridge National Laboratory, Oak Ridge, Tennessee 37831-6372
(Received 30 January 1991)

The projectile K Auger electron emission observed during grazing collisions of 60-keV N^{6+} ions with Au(110) is characterized by two components with strikingly different dependences on perpendicular velocity. A "fast" component dominates and is ascribed to "subsurface" emission. This component was satisfactorily modeled using a Monte Carlo simulation of the projectile trajectories *after* surface penetration. A "slow" component appears at very small angles and has a time dependence characteristic of the neutralization-deexcitation cascade predicted to occur above the surface *prior* to bulk penetration.

PACS numbers: 79.20.Nc, 34.70.+e, 79.90.+b

The interaction of multiply charged ions with metal surfaces has become a topic of intense experimental study (e.g., Refs. [1–4]). One of the interesting and unexpected results that has emerged from these recent studies is that remarkably rapid neutralization of the highly charged projectiles occurs. Previous investigations [2–4] of electron emission for slow incident ions of intermediate charge states ($q < 10$) have suggested that this neutralization occurs *prior* to penetration of the surface. This inference was based on two experimental observations. First, for slow projectiles carrying inner L- or K-shell vacancies, e.g., for Ar^{9+} or N^{6+} incident ions, respectively, projectile L or K Auger electrons are emitted with energies in the same range as those observed subsequent to L- or K-shell photoionization of neutral atoms. Second, the emitted electrons display Doppler shifts as a function of observation angle that are consistent with emission on the incident trajectory, i.e., prior to appreciable projectile angular scattering in the bulk material. In the present investigation, we have found that the latter observation is a necessary but not sufficient condition for proving that the Auger electron emission occurs *above* the surface.

The experimentally observed rapid and complete neutralization of multicharged ions which was interpreted as occurring above the surface is in strong disagreement with the frequently invoked model of multicharged ion neutralization near surfaces proposed by Arifov *et al.* [5] to explain the linear relationship observed between electron yield and total neutralization energy of the projectile multicharged ion. In this model, the primary neutralization mechanism is above-surface multiple resonant electron capture of metal valence electrons into autoionizing projectile Rydberg levels which decay preferentially by the emission of low-energy (15–30 eV) electrons, thus dissipating the total neutralization energy of the ion in a large number of small steps. This complex autoionization cascade requires time scales long compared to normal K Auger lifetimes [6], and thus is at odds with the experimentally inferred rapid and therefore almost complete neutralization of the projectile outer shells prior to K Auger decay.

We show in the present Letter that this discrepancy is resolved if the dominant contribution to the overall K Auger electron emission spectral line shape and intensity, previously ascribed to above-surface processes, is in fact due to "subsurface" emission. This conclusion is supported by a significant body of experimental data, for both Au and Cu single-crystal targets, which will be presented in its entirety in a lengthier contribution [7]. We have been able to successfully model the subsurface contribution to K Auger electron emission using a Monte Carlo simulation of the detailed projectile trajectories in the target. In the bulk, projectile neutralization by electron capture from loosely bound core and valence-band target levels proceeds on a time scale significantly faster than that required for K Auger decay. The K Auger emission therefore occurs with only small delay and, because of the statistical nature of the process, has a distribution of Auger electron energies corresponding to all different possible charge states, but peaked close to the neutral. At exceedingly small perpendicular velocities (i.e., very long above-surface interaction times), an additional, clearly resolvable, spectral feature appears which we ascribe to "above-surface" K Auger emission. The interaction-time dependence of this feature's intensity is in reasonable agreement with a calculation based on a numerical simulation of the deexcitation "ladder" implied by the Arifov model.

The experimental apparatus and technique has already been described elsewhere [4]. Briefly, a 60-keV N^{6+} ion beam extracted from the ORNL ECR ion source was magnetically analyzed and then collimated by passage through two small apertures to give a 1-mm-diam spot size on target at normal incidence, with a roughly 0.3° angular divergence. The target used was a clean Au(110) single crystal mounted on an x-y-z manipulator located in a UHV chamber with a base pressure of 5×10^{-10} Torr. Electron spectra were measured at 90° to the beam direction for angles of incidence in the range 0.5°–19.5° using a small spherical-sector energy analyzer with a nominal energy resolution of 2.8% and equipped with a multichannel-plate particle detector operated in the pulse counting mode. A Helmholtz coil arrangement was used to cancel stray magnetic fields in the region of the target crystal. The electron spectrometer pass energy and data collection were controlled by a microcomputer-based multichannel scaler. The dwell time per channel was determined by target current integration to a preset

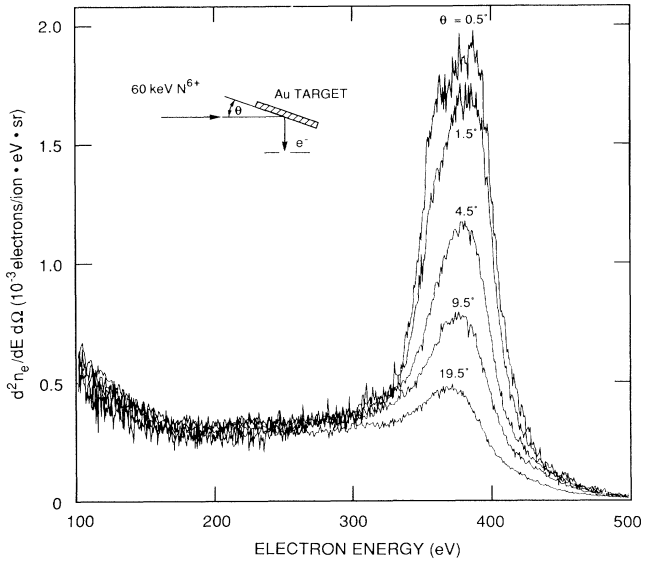

FIG. 1. Absolute projectile K Auger electron spectra measured for 60-keV N^{6+} ions incident on a Au target at five different angles.

accumulated charge. As previously described [4], the ion beam current intercepted by the second collimation aperture was used to normalize the measured electron spectra to the incident beam intensity. To permit an absolute comparison of the different electron spectra obtained, a geometric correction factor was applied for angles of incidence less than about 15° when the Au target region illuminated by the incident beam was larger than the experimentally determined viewing region of the electron spectrometer.

Using this approach, we have obtained the electron spectra shown in Fig. 1. With the exception of the channel-plate electron detection efficiency, which was assumed to be 40%, all the parameters required to put the doubly differential electron yields on an absolute scale were either determined experimentally or obtained from the known geometry and dimensions of our apparatus.

We focus first on the evolution of the shape of the projectile K Auger peak near 370 eV as a function of the angle at which the projectiles are incident on the Au target. Figure 2(a) shows the background-subtracted K Auger peaks, all scaled to the same peak height. The backgrounds were estimated by a sixth-order semilogarithmic (i.e., logarithmic in abscissa, linear in ordinate) polynomial fit using as "windows" those spectral regions dominated by continuum background. As can be seen from the figure, as the angle of incidence is decreased from 19.5° to 4.5°, the K Auger peak intensities increase (note scale factors to the left of each peak), while the spectral

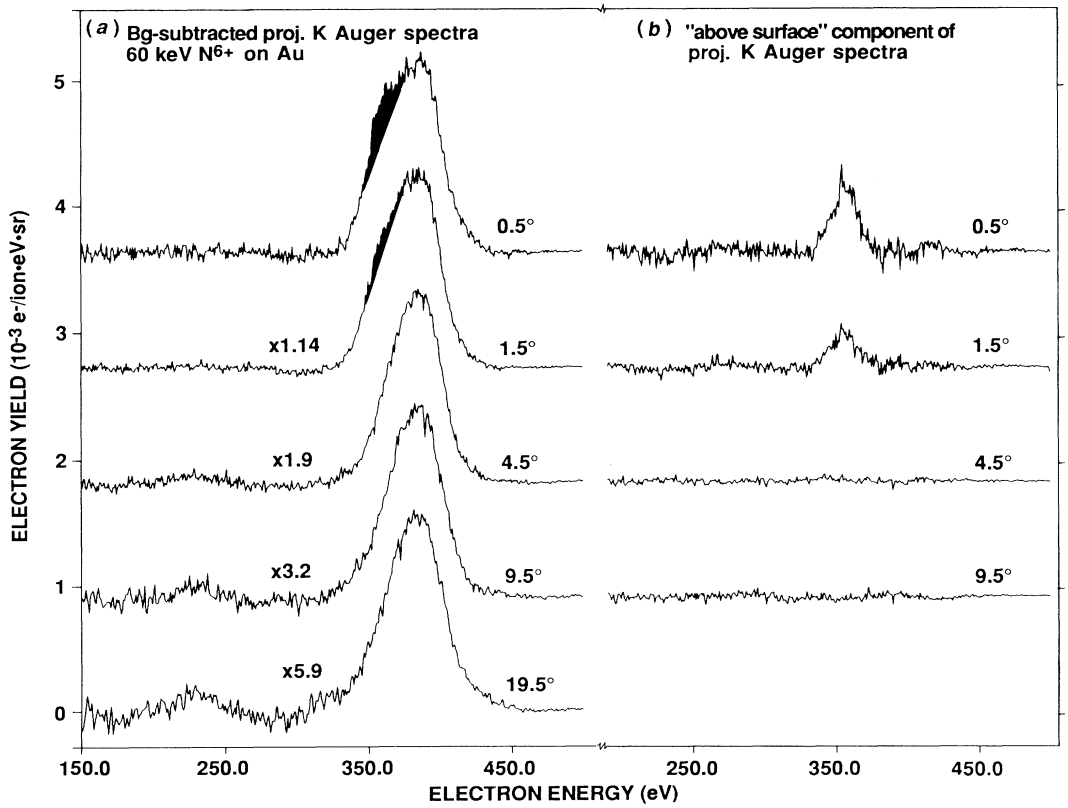

FIG. 2. (a) Background-subtracted projectile K Auger spectra scaled to the peak intensity of the 0.5° spectrum; the peak near 225 eV is an Au NNV transition, due to K-vacancy transfer from the projectile. (b) Unscaled above-surface components of the K Auger electron spectra.

shapes remain virtually unchanged. Starting with the 1.5° spectrum, a small feature [highlighted in black in Fig. 2(a)] is seen to appear on the low-energy slope of the main peak, which becomes more prominent in the 0.5° spectrum. The presence of this lower-energy component in the overall K Auger peak shape is more apparent in Fig. 2(b), where the main peak represented by the shape of one of the large-angle spectra has been subtracted. This subtraction procedure is based on the assumption that the main component of each of the spectra arises from the same mechanism. The total integrated intensity and the integrated intensity of the lower-energy component are shown in Fig. 3 as a function of inverse perpendicular velocity.

We ascribe the main component of the projectile K Auger peak to subsurface emission. This conclusion has been reached as a result of extensive Monte Carlo simulations of the projectile trajectories inside the solid target using the MARLOWE code [8]. A model was developed [7] in which the deexcitation of the projectile is assumed to progress in three sequential stages, consisting of the initial stage in which the projectile carries a K vacancy and has an empty L shell, an intermediate stage in which the K vacancy still survives, but the L shell has become (nearly) filled, and a final stage in which the K vacancy has decayed. The coupled differential equations describing the time evolution of this system are numerically integrated along the calculated projectile trajectories assuming a given L-shell filling rate R_L and K Auger decay rate R_K to determine total projectile K Auger electron production. The simulation is started at 3 atomic units above the surface plane The description of the projectile

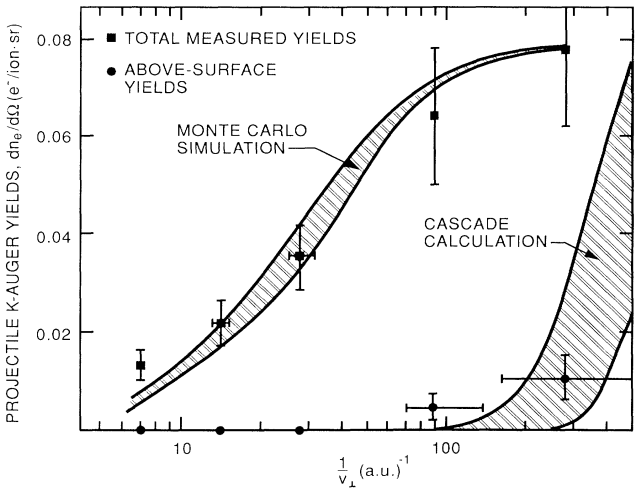

FIG. 3. Differential electron yields $dn_e/d\Omega$ for projectile K Auger emission normal to the incident beam direction as a function of inverse perpendicular projectile velocity. Solid squares, total measured yields; solid circles, experimentally deduced above-surface components; the hatched regions labeled "Monte Carlo" and "cascade" are numerical simulations of the subsurface and above-surface components of the K Auger emission, respectively (see text).

L-shell filling in terms of a continuous, macroscopic rate R_L is a simplifying, yet physically reasonable, approximation that is based on the assumption that the predominant L-shell filling mechanism is (multiple) electron capture from only semilocalized valence-band levels of the metal target. Initially, capture is most likely into the M shell of the projectile, and, in later neutralization stages, directly into the L shell (the rapid LMM Auger decay that follows the multiple-electron capture into the M shell is assumed to be contained in R_L). K-vacancy transfer in close binary collisions is incorporated into the simulation to permit calculation [7] of target Auger electron production [9]. In addition to the total Auger electron production, the fraction of electrons that escape the metal in a specified direction without inelastic scattering is determined by accumulating the incremental electron yield along each path segment weighted by the escape probability $\exp[-z/\cos(\theta)\lambda]$, where z is the depth below the surface, θ is the angle of observation relative to the surface normal, and λ is the electron inelastic mean free path. Doppler broadening effects due to angular scattering and straggling of the projectiles in the bulk prior to K Auger electron emission are accounted for in the model [7] by employing the local projectile velocity vector in the transformation required to obtain the laboratory frame energies of the electrons emitted by the projectile.

The hatched region labeled "Monte Carlo" in Fig. 3 shows the range of calculated differential yields of K Auger electrons that escape in the direction of observation obtained for different azimuthal incidence angles and various assumptions about the extent of surface damage [7], since neither of these parameters were precisely determined in the experiment. The inelastic mean free path for the ~370-eV N K Auger electrons was taken [10] to be 6 Å. The K Auger rate R_K used was 1×10^{14} s^{-1}, and is close to the tabulated [11] rate for neutral nitrogen. The L-shell filling rate R_L used was 2×10^{14} s^{-1}, and was determined by a fit to the data. As can be seen from the figure, the simulation reproduces the angular dependence of the measured electron yields reasonably well.

The validity of our interpretation of the main K Auger component as subsurface emission is further supported by three observations. First, from our simulation of detailed spectral line shapes [7], we find that the Doppler broadening due to projectile angular scattering or reflection prior to K Auger decay results in only subtle modifications of the peak shapes. These modifications are difficult to discern in the measured spectra (Fig. 1) due to the presence of continuum background [7] whose energy dependence is not precisely known. This indicates that little appreciable projectile angular scattering and straggling occur at depths less than the (1–2)λ escape depth of the K Auger electrons. As a result, the electrons emitted below the surface that escape without being inelastically scattered appear to have been emitted on the initial projectile trajectory, as has been previously inferred [2,3].

Second, because of the factor-of-2 smaller inelastic mean free path [10] for the lower-energy *LMM* Auger electrons, their probability of escape from a given depth of the solid without inelastic scattering is significantly smaller than that for the *K* Auger electrons. Partly as a result of this effect, the observed yield of *L* Auger electrons at intermediate perpendicular velocities is smaller than would be expected for a (nearly) filled *L* shell (which the *K* Auger electron energy distributions imply), as has in fact been experimentally observed [3,6]. Third, it is noted that, in contrast to the Auger electron results, measurements of projectile x-ray emission intensity [12] have shown only a small dependence on the angle of incidence. This difference is easily reconciled if dominance of subsurface electron emission is assumed, due to the large differences in attenuation lengths for electrons and photons in solids.

We now turn to the smaller component in the *K* Auger peak that appears at the two smallest angles of incidence [see Fig. 2(b)]. We ascribe this component to above-surface neutralization via the deexcitation cascade of the Arifov model mentioned at the beginning of this Letter. Figure 3 shows the time evolution of the above-surface *K* Auger yield calculated using a numerical simulation [6] of this cascade. Briefly, the model assumes instantaneous resonant neutralization (i.e., capture of 6 electrons) of the projectile $n=7$ shell at a specified critical distance above the surface. This multiexcited, neutralized projectile is then allowed to deexcite by single autoionization steps (with atomic rates [13]), while maintaining neutrality by additional resonant capture into $n=7$. The time evolution of the resulting cascade is solved numerically. The simulation results are shown (hatched region labeled "cascade") for two different assumed critical distances (20 and 40 atomic units) above the surface at which classical overbarrier transitions become possible. The smaller critical distance (lower boundary of hatched region) is obtained by proper accounting of the image potential [14]. In the present model, use of the larger value (upper boundary) is equivalent to a doubling of all the autoionization rates in the cascade, which should take into account [6] a possible underestimation of the rates used in the calculations. As can be seen, the experimental yields are in reasonable agreement [15] with the calculated range of yields. It is noted that recent, more sophisticated calculations [16] that combine a more realistic over-the-barrier model of multiple resonant electron capture and resonant loss with the autoionization cascade show very good agreement with the experimental yields.

In contrast to the subsurface *K* Auger emission, which occurs subsequent to almost complete *L*-shell filling, the numerical cascade simulation predicts close to the minimum population of the *L* shell (i.e., close to 2) at the time of the *K* Auger decay, implying lower *K* Auger electron energies than those characterizing the subsurface emission. This displacement is in fact evident in the measurements, where a shift of about 25 eV is noted. The peak position of the above-surface component of 350 eV implies [13] an *L*-shell population of 2 to 3, if it is assumed that the remaining electrons of the neutralized projectiles are distributed in the *M* and higher shells. Similar differences in *L*-shell populations have been noted [12,17] for above-surface versus subsurface $K\alpha$ x-ray emission during multicharged-ion–surface interactions.

We gratefully acknowledge the advice and help of M. T. Robinson in performing the Monte Carlo simulations. This research was supported by the Division of Chemical Sciences, Office of Basic Energy Sciences, and by the Division of Applied Plasma Physics, Office of Fusion Energy, of the U.S. Department of Energy, under Contract No. DE-AC05-84OR21400 with Martin Marietta Energy Systems, Inc.

[1] J. P. Briand, L. de Billy, P. Charles, S. Essaba, P. Briand, R. Geller, J. P. Desclaux, S. Bliman, and C. Ristori, Phys. Rev. Lett. **65**, 159 (1990).

[2] S. T. de Zwart, A. G. Drentje, A. L. Boers, and R. Morgenstern, Surf. Sci. **219**, 298 (1989); S. T. de Zwart, Ph.D. thesis, Groningen University, 1987 (unpublished).

[3] L. Folkerts and R. Morgenstern, Europhys. Lett. **13**, 377 (1990).

[4] F. W. Meyer, C. C. Havener, S. H. Overbury, K. J. Reed, K. J. Snowdon, and D. M. Zehner, J. Phys. (Paris), Colloq. **50**, C1-263 (1989).

[5] U. A. Arifov, L. M. Kishinevskii, E. S. Mukhamadiev, and E. S. Parilis, Zh. Tekh. Fiz. **43**, 181 (1973) [Sov. Phys. Tech. Phys. **18**, 118 (1973)].

[6] P. A. Zeijlmans van Emmichoven, C. C. Havener, and F. W. Meyer, Phys. Rev. A **43**, 1405 (1991).

[7] F. W. Meyer, S. H. Overbury, C. C. Havener, P. A. Zeijlmans van Emmichoven, J. Burgdörfer, and D. M. Zehner (to be published).

[8] M. T. Robinson, Phys. Rev. B **40**, 10717 (1989).

[9] F. W. Meyer, C. C. Havener, K. J. Snowdon, S. H. Overbury, and D. M. Zehner, Phys. Rev. A **35**, 3176 (1987).

[10] B. Lesiak, A. Jablonski, Z. Prussak, and R. Mrozek, Surf. Sci. **223**, 213 (1989); C. J. Tung, J. C. Ashley, and R. H. Ritchie, Surf. Sci. **81**, 427 (1979).

[11] M. O. Krause, J. Phys. Chem. Ref. Data **8**, 307 (1979).

[12] M. Schulz, C. L. Cocke, M. Stöckli, S. Hagmann, and H. Schmidt-Böcking, Z. Phys. D (to be published).

[13] R. D. Cowan, *The Theory of Atomic Structure and Spectra* (University of California Press, Berkeley, 1981).

[14] K. J. Snowdon, Nucl. Instrum. Methods Phys. Res., Sect. B **34**, 309 (1988).

[15] We note that in this comparison image-potential acceleration of the projectile during its approach to the surface has been ignored. Inclusion of this effect would increase the N^{6+} projectile's kinetic-energy component perpendicular to the surface by a minimum of about 12 eV. As a result, the yields for the smallest two nominal incidence angles, i.e., 1.5° and 0.5°, should more correctly be plotted at $1/v_\perp$ of 82 and 144 a.u.$^{-1}$, respectively.

[16] J. Burgdörfer, P. Lerner, and F. W. Meyer (to be published).

[17] J. J. Bonnet, A. Fleury, M. Bonnefoy, M. Chassevent, T. Lamy, A. Brenac, A. Simionovici, H. J. Andrä, and S. Andriamonje, Z. Phys. D (to be published).